

## Article

# Rare Earth Occurrence States of Weathered Crust Elution-Deposited Rare Earth Ores in Southern Yunnan

Wendou Chen <sup>1</sup>, Zhenyue Zhang <sup>1,2,\*</sup>, Fei Long <sup>1</sup>, Zhuo Chen <sup>1</sup> and Ru'an Chi <sup>1,2</sup><sup>1</sup> School of Resources & Safety Engineering, Wuhan Institute of Technology, Wuhan 430073, China<sup>2</sup> Key Laboratory for Green Chemical Process of Ministry of Education, Wuhan Institute of Technology, Wuhan 430073, China

\* Correspondence: zyzxmu@wit.edu.cn; Tel.: +86-13419645585

**Abstract:** To reveal the regularity of variation in the rare earth occurrence states of weathered crust elution-deposited rare earth ores, ore samples from different weathering crust layers were obtained by performing the sequential extraction procedure. The order of rare earth contents firmly obeyed the following sequence: the weathered layer > humic layer > partly weathered layer. The occurrence states of rare earth elements were mainly the ion exchange state, carbonate bound state, iron–manganese oxide state, organic binding state and residual state. The proportions of rare earth elements found in the rare earth ion exchange state of the weathered layer, humic layer and partly weathered layer were 78.55%, 73.53% and 53.88%, respectively. The light rare earth elements (LREEs) found in the rare earth ion exchange state were enriched in the upper part of the weathering crust, while the heavy rare earth elements (HREEs) were enriched in the lower part. There were also obvious negative anomalies in the content of cerium in the ion exchange state. The content of rare earth elements found in the carbonate bound state was small, and the rare earth partition pattern was basically consistent with that of the ion exchange state, which had little effect on the differentiation of the rare earth elements. The iron–manganese oxide state was mainly enriched with cerium, and the content of cerium increased with the depth of the weathering crust. The iron–manganese oxide state was the main factor causing the phenomenon of the anomaly in the cerium content. Meanwhile, the iron oxides in the iron–manganese oxide state were mainly hematite and goethite. The organic binding state mainly beneficiated yttrium and cerium by complexation and certain adsorption. The content of elements found in the rare earth residual state was related to the degree of weathering and reflected the release sequence of rare earth elements in the mineralization process. Clarifying the rare earth occurrence states is conducive to better revealing the metallogenic regularity of weathered crust elution-deposited rare earth ores. In addition, the results can provide a valuable reference for expanding the available rare earth resources and the efficient comprehensive utilization of rare earth ore.



**Citation:** Chen, W.; Zhang, Z.; Long, F.; Chen, Z.; Chi, R. Rare Earth Occurrence States of Weathered Crust Elution-Deposited Rare Earth Ores in Southern Yunnan. *Minerals* **2023**, *13*, 554. <https://doi.org/10.3390/min13040554>

Academic Editor: Saeed Chehreh Chelgani

Received: 13 March 2023

Revised: 2 April 2023

Accepted: 12 April 2023

Published: 14 April 2023

**Keywords:** weathered crust elution-deposited rare earth ores; rare earth; occurrence state; ion exchange state; iron–manganese oxide state



**Copyright:** © 2023 by the authors. Licensee MDPI, Basel, Switzerland. This article is an open access article distributed under the terms and conditions of the Creative Commons Attribution (CC BY) license (<https://creativecommons.org/licenses/by/4.0/>).

## 1. Introduction

Weathered crust elution-deposited rare earth ores are rich in medium and heavy rare earth elements; thus, they have high economic value and are strategic mineral resources in China [1–3]. This mineral was firstly discovered in the Jiangxi province of China, and is mainly located in the Jiangxi, Fujian, Hunan, Guangdong, Guangxi and Zhejiang provinces [4,5]. In recent years, large medium-heavy rare earth deposits have been discovered in southern Yunnan [6], with the characteristics of high altitude, diverse metallogenic models, large differences in the rare earth element content distribution, and a diverse and complex terrain. These characteristics lead to such problems as a large difference in the rare earth grade, the complex distribution of the rare earth enrichment area, the poor stability of

the ore body and the presence of many blind areas of leaching. In a warm humid climate, the rocks originally containing the rare earth minerals are weathered and converted to clay minerals by biological, chemical and physical processes, and the rare earth elements are primarily absorbed into the clay minerals in the form of hydrated ions or hydrated hydroxyl ions [7,8]. The weathered crust elution-deposited rare earth orebody is divided into three weathering crust layers (Figure 1) from top to bottom, according to the degree of weathering [9–11].

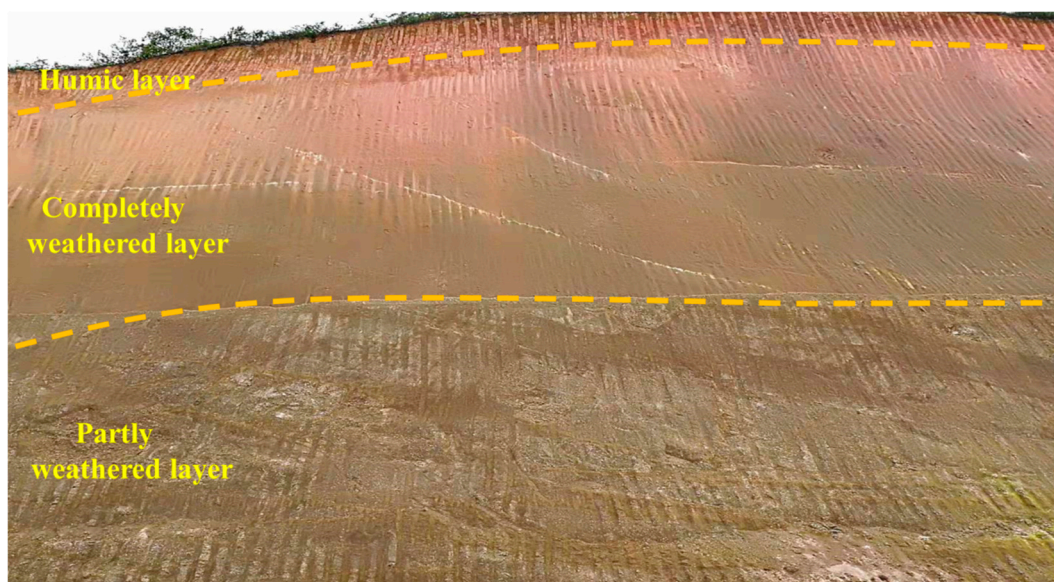


**Figure 1.** Profile of weathered crust elution-deposited rare earth ore body.

Rare earth fractionation occurs in different weathering crust layers through the dissolution of rare earth element (REE)-bearing minerals [12,13]. This process includes the formation of rare earth secondary minerals, the formation of complex organic and inorganic materials, the adsorption and desorption of rare earth elements, an oxidation reduction reaction and the precipitation of rare earth elements [14–17]. Rare earth elements are mainly enriched in the lower part of the weathered layer as secondary minerals or are adsorbed on clay minerals and Fe–Mn oxides [18–21]. Weathered crust elution-deposited rare earth ores contain 50% to 90% ion-exchangeable REEs, predominantly on the surface of kaolinite and halloysite [22]. Meanwhile, apart from the ion exchangeable state, rare earth elements are also found in the Fe–Mn (hydrogen) oxide state, residual state, organic binding state and carbonate bound state [23,24]. Studies on the occurrence state of ore have revealed some of the effective means by which to efficiently utilize ore. Many scientists and technologists have conducted extensive research on the occurrence of rare earth elements in weathered crust elution-deposited rare earth ore, and have achieved many significant results. Fan et al. [25] studied the rare earth element carrier minerals in deep sea sediments and showed that the dominant carrier minerals in the deep-sea sediments of the Pacific and Indian oceans include apatite, ferromanganese oxides (hydroxide), clay minerals, and phillipsite. They found that rare earth element and yttrium (REY) entered into the apatite structure in the form of coupled substitution, and that in ferromanganese nodules, the REY occurred mainly in the form of surface complexation and adsorption. Wang et al. [26] conducted a comparative study on the geochemical characteristics of rare earth elements in the deep-sea sediments of different areas of the Pacific Ocean. The results showed that the contents of REY in deep-sea sediments in the central and northwestern pacific, especially in zeolite clay, were generally significantly higher than those in the eastern Pacific polymetallic mud. The REY contents in zeolite clay and pelagic clay were mainly related to phosphate. The CaO/P<sub>2</sub>O<sub>5</sub> ratios in supernormally high REY sediments tended to be consistent and almost

close to the CaO/P<sub>2</sub>O<sub>5</sub> ratios of the apatite. Wood S.A. et al. [27] studied the geochemical behavior of rare earth ions in solution and found that in an acidic environment (pH < 4), rare earth elements were mainly free ions in the organic environment. When they meet groundwater with high F<sup>-</sup> and SO<sub>4</sub><sup>2-</sup>, part of the rare earth element migrates in the form of fluorine and sulfate complexes. With the increase in the pH of the soil solution and groundwater, the rare earth elements, especially the heavy rare earth elements, transform into the carbonate complex, and the rare earth element and carbonate complex migrate with the groundwater. Studies on the occurrence of rare earth elements in soil, ocean and low-altitude mines have been relatively complete [28–30]. However, there have been few reports on the rare earth occurrence states that are present in this high-altitude metallogenic model in southern Yunnan. The variety of rare earth occurrence states determines the mining method and the choice of reagents used. Clarifying the occurrence states of rare earth elements in high-altitude rare earth minerals not only enriches the theoretical knowledge, but also helps to guide the use of beneficiation agents. Therefore, urgent research on the rare earth metallogenic model and the occurrence state characteristics of rare earth elements in high-altitude weathered crust elution-deposited rare earth ores has been required for some time.

Therefore, the rare earth occurrence states of weathered crust elution-deposited rare earth ores in southern Yunnan were studied in this paper. The aim of this study was to explore the occurrence of rare earth elements in the humic layer, completely weathered layer and partly weathered layer of weathered crust elution-deposited rare earth ores. At the same time, the abnormal phenomena and the occurrence form of the rare earth element cerium in the iron–manganese oxide state and the abnormal phenomena of the rare earth element yttrium in the organic binding state were studied. As such, the ore-forming mechanism and the occurrence state of rare earth elements found in the weathered crust elution-deposited rare earth ores of southern Yunnan were further revealed. This study is helpful in that it clarifies the rare earth occurrence state of weathered crust elution-deposited rare earth ores to better guide the mining of rare earth minerals and beneficially improve the efficient utilization of rare earth resources.

## 2. Materials and Methods

### 2.1. Experimental Scheme and Principle

The ore samples were collected from southern Yunnan. A sufficient amount of rare earth ore was taken from the three weathering crust layers and dried for 8 h at 50 °C in an electric heating constant-temperature blow-drying oven. In total, 25 g of ore sample was taken into a beaker for the sequential extraction procedure experiment [31]. The sequential extraction procedure was used to obtain the different occurrence states of rare earth elements. The rare earth occurrence states were divided into the ion exchange state (Ion-Ex), carbonate bound state (Carbonate), iron–manganese oxide state (Fe–Mn), organic binding state (Organic) and residual state (Residual). The same batch of samples was tested three times in parallel, and the obtained solution was mixed evenly before the sample was measured in order to eliminate the influence of experimental errors. The concentrations and partition characteristics of the rare earth elements in each occurrence state were determined using ICP-MS.

The mineralogical composition of the sample was identified using X-ray diffraction (D8 ADVANCE, Cu-K $\alpha$  radiation in the range of 10 to 90°2 $\theta$  with a scanning speed of 2.4°2 $\theta$ /min). The chondrite standard values of rare earth elements were analyzed using the standard values recommended by Boynton (1984). Scanning electron microscopy and energy spectrum (SEM-EDS) images were obtained using a Zeiss Gemini SEM300 equipped with an energy-dispersive X-ray spectrograph. Transmission electron microscopy (TEM) images were obtained using JEM 2100 instruments from Japan Electronics.

The outliers of REE can be quantified by  $\delta\text{REE}$ . Taking the calculation of cerium outliers as an example, the calculation formula was as follows:

$$\delta\text{Ce} = \frac{\text{Ce}}{\text{Ce}^*} = \frac{\text{Ce}_N}{\sqrt{\text{La}_N \times \text{Pr}_N}}$$

In the formula,  $\text{Ce}^*$  represents the content of Ce when it was not abnormal.  $\text{Ce}_N$ ,  $\text{La}_N$  and  $\text{Pr}_N$  represent the chondrite standardized values of the measured values of this element. When the outlier was less than 0.95, it was a negative anomaly, and when the outlier was greater than 1.05, it was a positive anomaly [32].

All the reagents used in the experiment were analytically pure, and all the solutions used in the experiment were prepared with deionized water.

## 2.2. Ore Properties of Rare Earth Ore Samples

The ore samples used in the experiment were collected from southern Yunnan, China. The chemical composition of the ore sample was determined using XRF (X-ray fluorescence spectrometry) [33], and the results are shown in Table 1.

**Table 1.** Main chemical composition of the RE ores/%.

Composition	Content		
	Humic Layer	Completely Weathered Layer	Partly Weathered Layer
REO	0.177	0.278	0.149
Al <sub>2</sub> O <sub>3</sub>	32.212	30.509	22.358
CaO	0.071	0.062	0.106
SiO <sub>2</sub>	58.997	60.658	67.185
MnO <sub>2</sub>	0.108	0.136	0.386
ZnO	0.031	0.028	0.018
MgO	0.325	0.659	0.541
P <sub>2</sub> O <sub>5</sub>	0.098	0.115	0.109
K <sub>2</sub> O	3.510	4.103	4.569
SO <sub>3</sub>	0.134	0.098	0.188
TiO	0.112	0.108	0.098
Fe <sub>2</sub> O <sub>3</sub>	1.659	1.436	1.058
Rb <sub>2</sub> O	0.017	0.028	0.038
SrO	0.009	0.015	0.045
ZrO <sub>2</sub>	0.017	0.014	0.024
Na <sub>2</sub> O	0.062	0.515	1.021
Loss	2.461	1.238	2.107

It can be seen from Table 1 that the SiO<sub>2</sub> content was the highest in each weathered layer, followed by Al<sub>2</sub>O<sub>3</sub>. The order of the rare earth oxide (REO) content in each weathered layer rigidly obeyed the following sequence: weathered layer > humic layer > partly weathered layer, with REO contents of 0.278%, 0.177% and 0.149%, respectively. To analyze the composition of the weathered crust elution-deposited rare earth ore, the fine-grained ore obtained from the three weathering crust layers was tested using X-ray diffraction, and the results are shown in Figure 2.

It can be seen from Figure 2 that the main components of the rare earth ore were quartz, kaolinite group minerals and illite group minerals. By comparing the ore to the standard portable document format (PDF) card library, it can be determined that it conforms to the card PDF#46-1045 (Quartz, SiO<sub>2</sub>).

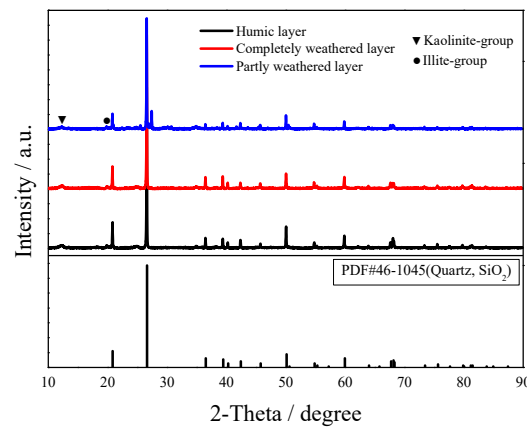


Figure 2. The XRD pattern of rare earth ore.

### 3. Results and Discussion

#### 3.1. Occurrence State of RE on Weathered Crust Elution-Deposited Rare Earth Ores

To reflect the rare earth occurrence states in each weathered layer, the proportions of the rare earth occurrence states in the three weathering crust layers were calculated, and the results are shown in the Figure 3.

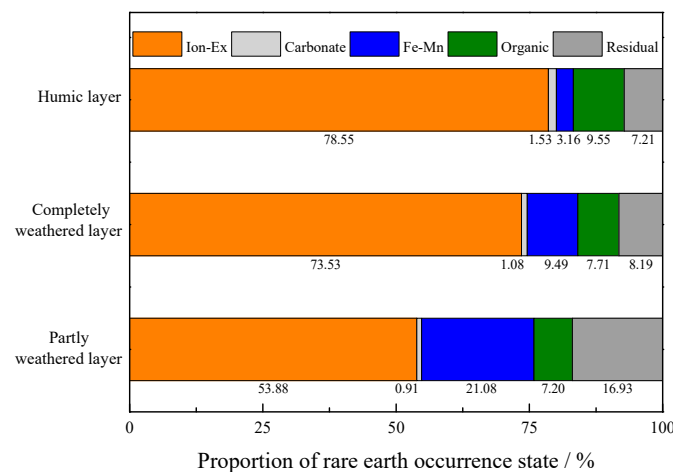


Figure 3. Proportion of rare earth occurrence state in each weathered layer.

It can be seen from Figure 3 that the contents of rare earth elements in the rare earth ion exchange state were the highest in each weathered layer, with proportions of 78.55%, 73.53% and 53.88% respectively. This was because the weathering degree of the weathering profile from top to bottom gradually weakens. The content of the rare earth carbonate bound state was small, and hardly affected the differentiation of the rare earth elements, and the average proportion was only 1.17%. The contents of rare earth elements in the iron–manganese oxide state increased gradually with the deepening of the weathering crust profile, and were 3.16%, 9.49% and 21.08%, respectively. Therefore, it can be seen that iron–manganese oxide had an important effect on the differentiation of the rare earth elements. The iron and manganese oxides were complex forms of particles and clay minerals. With the weathering of the ore bodies, the iron and manganese oxides migrated downward, resulting in an increase in the iron and manganese oxides in the lower part of the weathering crust. The content of rare earth elements in the organic binding state in the weathering crust profile decreased gradually with the deepening of the profile depth, and the proportions of rare earth elements in the organic binding state in each weathered layer were 9.55%, 7.71% and 7.20%, respectively. This was because the closer the weathering crust was to the earth’s

surface, the more organic matter there was, such as humic acid in the humic layer; a large number of plant roots led to a rise in organic matter content in the environment, resulting in an enhancement in the organic binding rare earth content [34]. The contents of rare earth elements in the residual state were related to the degree of weathering. The contents of rare earth elements in the residual state increased gradually from the top to the bottom of the weathering profile, and were 7.21%, 8.19% and 16.93%, respectively. Due to the decrease in the weathering degree, content of the secondary minerals formed decreased, and the residual minerals mainly inherited the original rock.

### 3.2. Concentrations of Rare Earth in Weathering Crust Layers in Different Occurrence States

Rare earth occurrence states in each weathered layer were obtained by using the sequential extraction procedure. The concentrations of rare earth elements in different occurrence states were detected using ICP-MS, and the results are shown in Table 2.

**Table 2.** Rare earth concentrations in different occurrence states/ $\mu\text{g}\cdot\text{g}^{-1}$ .

Weathered Layer	Occurrence States	La <sub>2</sub> O <sub>3</sub>	CeO <sub>2</sub>	Pr <sub>6</sub> O <sub>11</sub>	Nd <sub>2</sub> O <sub>3</sub>	Sm <sub>2</sub> O <sub>3</sub>	Eu <sub>2</sub> O <sub>3</sub>	Gd <sub>2</sub> O <sub>3</sub>	Tb <sub>2</sub> O <sub>3</sub>	Dy <sub>2</sub> O <sub>3</sub>	Ho <sub>2</sub> O <sub>3</sub>	Er <sub>2</sub> O <sub>3</sub>	Tm <sub>2</sub> O <sub>3</sub>	Yb <sub>2</sub> O <sub>3</sub>	Lu <sub>2</sub> O <sub>3</sub>	Y <sub>2</sub> O <sub>3</sub>	∑LREEs	∑HREEs	∑REO	LREEs/HREEs
Humic layer	Ion-Ex	491.54	130.27	125.68	407.75	69.89	6.94	33.61	4.00	23.23	3.73	9.55	1.27	8.04	1.09	92.61	1155.24	253.96	1409.20	4.55
	Carbonate	9.34	1.09	2.43	7.82	1.51	0.11	0.72	0.06	0.59	0.09	0.27	0.04	0.22	0.02	2.08	20.68	5.71	26.39	3.62
	Fe-Mn	10.68	29.28	1.89	9.51	0.99	0.14	0.64	0.05	0.69	0.13	0.34	0.04	0.33	0.05	2.35	51.36	5.75	57.11	8.93
	Organic Residual	14.53	61.34	2.69	18.35	1.81	0.13	0.72	0.12	0.59	0.18	0.26	0.10	0.20	0.08	53.34	96.91	57.53	154.44	1.68
Completely weathered layer	Ion-Ex	766.19	9.52	184.06	569.92	121.66	10.95	81.97	10.23	61.37	10.65	32.11	5.18	28.16	3.15	320.65	1529.69	686.08	2215.77	2.23
	Carbonate	9.54	0.04	2.81	7.89	1.76	0.13	1.14	0.13	1.03	0.15	0.51	0.08	0.49	0.05	4.20	20.28	9.67	29.95	2.10
	Fe-Mn	20.66	118.72	3.42	17.98	2.39	0.12	1.29	0.12	1.78	0.10	0.96	0.14	1.01	0.16	7.71	160.78	15.78	176.56	10.19
	Organic Residual	15.23	30.31	3.93	15.46	3.38	0.39	2.16	0.32	2.15	0.30	1.12	0.11	0.62	0.12	81.54	64.93	92.21	157.14	0.70
Partly weathered layer	Ion-Ex	137.99	21.83	20.45	107.09	21.61	2.54	32.24	6.52	44.28	8.83	27.42	4.24	26.22	3.89	308.95	287.36	486.74	774.10	0.59
	Carbonate	1.63	0.12	1.90	1.27	0.31	0.05	0.59	0.17	1.00	0.44	1.18	0.52	0.97	0.37	3.56	4.92	9.16	14.08	0.54
	Fe-Mn	27.23	211.93	5.87	46.06	3.22	0.25	2.26	0.22	2.52	0.58	1.20	0.24	1.26	0.21	9.52	291.09	21.48	312.57	13.55
	Organic Residual	17.50	36.62	3.12	14.93	1.92	0.21	1.48	0.19	1.38	0.17	0.64	0.14	0.47	0.12	50.92	72.17	57.64	129.81	1.25
Partly weathered layer	Ion-Ex	86.88	45.30	20.14	32.42	8.30	0.49	7.15	1.29	4.38	1.21	2.52	0.36	3.79	0.92	43.01	184.74	73.42	258.16	2.52
	Carbonate																			
	Fe-Mn																			
	Organic Residual																			

Table 2 shows the variations in the content of rare earth elements under different weathering layers and different occurrence states. It can be seen from Table 2 that the variation in the content of rare earth elements conformed to the Oddo–Harkins rule. According to the content distribution of rare earth elements in various occurrence states, ion exchange states were the main binding forms, and the values of the weathered layer > humic layer > partly weathered layer sequence were 2215.77  $\mu\text{g}\cdot\text{g}^{-1}$ , 1409.20  $\mu\text{g}\cdot\text{g}^{-1}$  and 774.10  $\mu\text{g}\cdot\text{g}^{-1}$ , respectively. However, the enrichment ratio of LREEs/HREEs in the rare earth ion exchange state varied greatly. From the humic layer to the partly weathered layer, the LREEs/HREEs were 4.55, 2.23 and 0.59, respectively. Therefore, the lower part of the weathering crust was enriched in more heavy rare earth elements than the upper part. At the same time, it can be seen that the content of the rare earth element cerium in the iron–manganese oxide state had an obvious abnormal effect, and there were also some abnormal corresponding rare earth elements, cerium and yttrium, in the organic binding state. The ratios of LREEs/HREEs in the iron–manganese oxide state gradually increased from the humic layer to the partly weathered layer, and were 8.93, 10.19 and 13.55, respectively, which was caused by the abnormal enrichment of the element cerium. However, due to the abnormal enrichment of yttrium in the organic binding state, the LREEs/HREEs of different weathering layers were significantly abnormal, at 1.68, 0.70 and 1.25, respectively. This indicated that the organic binding state was enriched in the heavy rare earth elements more easily, especially Y. In order to accurately present the differentiation phenomenon of rare earth elements in different weathering crust layers and different occurrence states, the occurrence states of five rare earth elements are discussed in the following part.

### 3.3. Ion-Ex State of the Weathered Crust Elution-Deposited Rare Earth Ores

In order to elucidate the differentiation characteristics of the rare earth elements in the ion exchange state in different weathering crust layers, the contents and ratios of fifteen rare earth elements in ion exchange states were analyzed. The contents of rare earth elements in the ion exchange state are shown in Figure 4a, and the chondrite standard values of rare earth elements are shown in Figure 4b.

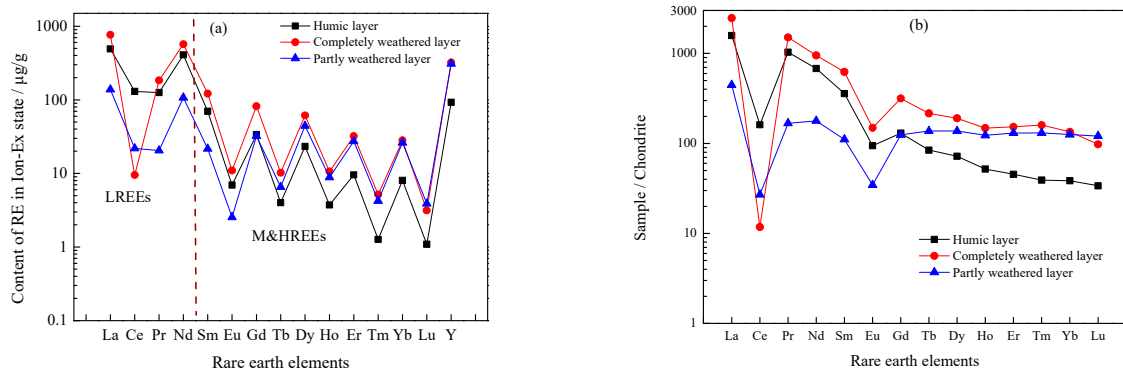


**Figure 4.** Rare earth contents and chondrite standard values of Ion exchange state. (a) Content of ion exchange state of rare earth elements in each weathered layer; (b) Standard for ion exchange state of rare earth element chondrites in each weathered layer.

It can be seen from Figure 4a that the total content of rare earth elements in the ion exchange state followed the order completely weathered layer > humic layer > partly weathered layer, and the main rare earth elements were La, Pr, Nd and Y. The content of M&HREEs in the humic layer was obviously lower than that in the other weathering crust layers, indicating that the migration rate of LREEs was obviously lower than that of M & HREEs, and that M & HREEs were more easily enriched and ore-formed in the lower part of the weathering crust. The average contents of LREEs from the humic layer to the partly weathered layer were  $288.81 \mu\text{g}\cdot\text{g}^{-1}$ ,  $382.42 \mu\text{g}\cdot\text{g}^{-1}$  and  $71.84 \mu\text{g}\cdot\text{g}^{-1}$ , respectively, and the average contents of M&HREE were  $23.09 \mu\text{g}\cdot\text{g}^{-1}$ ,  $62.37 \mu\text{g}\cdot\text{g}^{-1}$  and  $44.25 \mu\text{g}\cdot\text{g}^{-1}$ , which verified the fractionation effect in the rare earth mineralization process [11]. It can be seen from Figure 4b that there were certain cerium anomalies and europium anomalies in the different weathering crust layers of the weathered crust elution-deposited rare earth ore in southern Yunnan. The anomalous value of cerium was  $0.95 > \text{humic layer} > \text{partly weathered layer} > \text{completely weathered layer} > 0$ ; the results indicated that the ion exchange state of the rare earth elements in all the weathering crust layers in southern Yunnan encountered a negative anomaly regarding the content of cerium, especially in the completely weathered layer. This was because the element cerium had variable valence, and was easily formed a stable soluble complex with  $\text{HCO}_3^-$  in the water medium, which was then lost with the water medium, resulting in the differentiation and further loss of other rare earth elements [35]. The abnormal value of the element europium was relatively stable and mainly depended on the inherited parent rocks. Europium anomalies in parent rocks were often related to the crystallization of plagioclase in various magmatic rocks, because the distribution coefficient of plagioclase to europium in various minerals was much greater than that of other rare earth elements. In the process of magma separation crystallization, a large amount of plagioclase crystals removed europium, resulting in the formation of a certain europium negative anomaly in the residual melt [32].

### 3.4. Carbonate Bound State of the Weathered Crust Elution-Deposited Rare Earth Ores

Carbonate bound states mainly reflect the adsorption of elements on the surface of carbonate or co-precipitation. The rare earth carbonate bound state is a rare earth occurrence state in which rare earth ions combine with carbonate. The rare earth contents of the carbonate bound state in different weathering crust layers are shown in Figure 5.

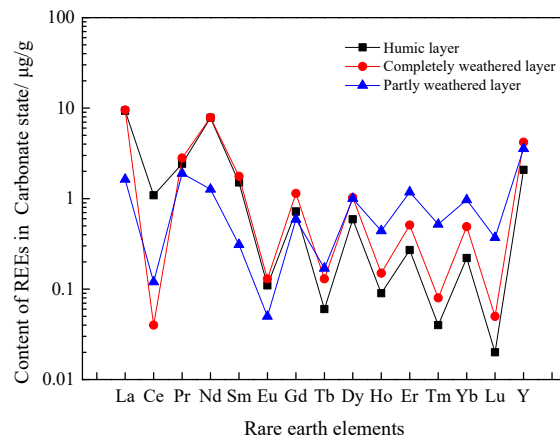


Figure 5. Rare earth contents of carbonate bound state.

It can be seen from Figure 5 that the content of rare earth elements in the carbonate bound state was very small, and the average values of rare earth elements in the carbonate bound state from the humic layer to the partly weathered layer were  $1.76 \mu\text{g}\cdot\text{g}^{-1}$ ,  $1.99 \mu\text{g}\cdot\text{g}^{-1}$  and  $0.94 \mu\text{g}\cdot\text{g}^{-1}$ , respectively, which had little influence on the differentiation of rare earth elements in the mineralization process. Compared with the distribution of rare earth elements in the ion exchange state, it can be seen that the rare earth distribution pattern in the carbonate bound state inherited the distribution of rare earth elements in the ion exchange state. The formation of the carbonate bound state rare earth was due to the formation of a stable  $\text{REECO}_3^+$  or  $\text{REE}(\text{CO}_3)_2^-$  complex between rare earth elements and carbonate. In the in situ leaching process of rare earth elements, due to the leaching effect of rain or a leaching agent, the rare earth carbonate bound state cannot exist stably under this condition. Therefore, the content of rare earth elements in the carbonate bound state was very small and had little influence on the differentiation of rare earth elements.

### 3.5. Fe–Mn Oxide State of the Weathered Crust Elution-Deposited Rare Earth Ores

Iron–manganese oxide was an important factor affecting REE differentiation during the mineralization of weathered crust elution-deposited rare earth ores. The contents of rare earth elements in the iron–manganese oxide state in different weathering crust layers are shown in Figure 6a, and the proportion of rare earth elements in the iron–manganese oxide state are shown in Figure 6b.

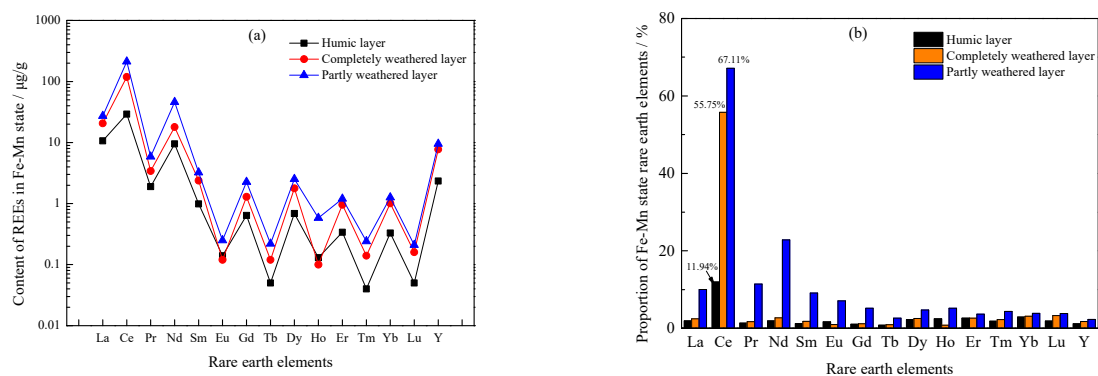


Figure 6. The rare earth content and proportion of iron–manganese oxide. (a) Content of Fe–Mn oxide state rare earth elements in each weathered layer; (b) The proportion of rare earth elements in the Fe–Mn oxide state of rare earth ore in each weathered layer.

As can be seen from Figure 6a, iron and manganese oxides were more enriched in LREEs, and mainly in cerium. The order of the content of REEs in the iron–manganese

oxide state in the different weathering crust layers was partly weathered layer > completely weathered layer > humic layer, and the contents were  $312.57 \mu\text{g}\cdot\text{g}^{-1}$ ,  $176.56 \mu\text{g}\cdot\text{g}^{-1}$  and  $57.11 \mu\text{g}\cdot\text{g}^{-1}$ , respectively. It can be seen from Figure 6b that the element cerium accounts for 55.75% and 67.11% of the completely the weathered layer and partly weathered layer, respectively; this was the reason for the depletion of the rare earth element cerium in the ion exchange state of the weathering crust layers, which thus presented the cerium anomaly effect.

In order to explain the abnormal content of the element cerium, the recommended value of Boynton (1984) was used as the chondrite standard of the iron–manganese oxide state, and the results are shown in Figure 7.

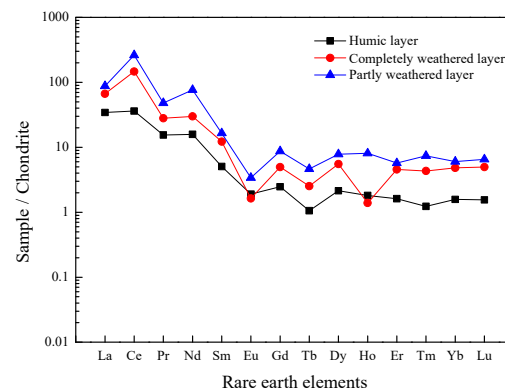


Figure 7. Chondrite standard of Fe–Mn state rare earth.

It can be seen from Figure 7 that there were obvious cerium anomalies in all weathering crust layers of the rare earth iron–manganese oxide state. The anomalous values of cerium in the different weathering crust layers were  $\delta_{\text{partly}} = 4.03 > \delta_{\text{completely}} = 3.40 > \delta_{\text{humic}} = 1.57 > 1.05$ , indicating that the element cerium of the iron–manganese oxide state in all the weathering crust layers presented an obvious positive anomaly phenomenon. Therefore, iron–manganese oxide was the main factor leading to the occurrence of the cerium anomaly. The specific adsorption of iron–manganese oxide on cerium was caused by the change in the valence of cerium. The adsorption process of iron–manganese oxide on cerium is shown in Figure 8.

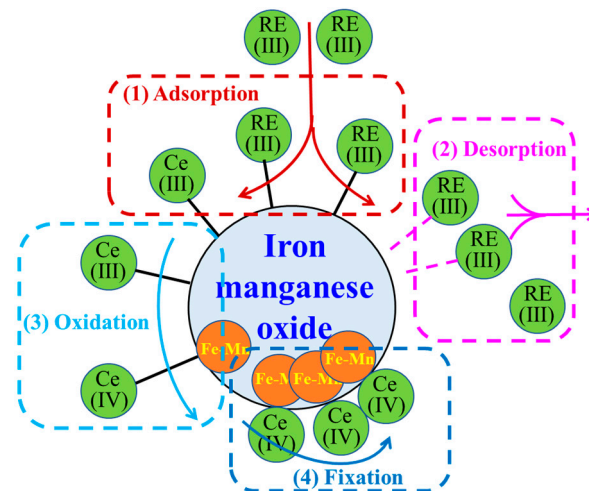
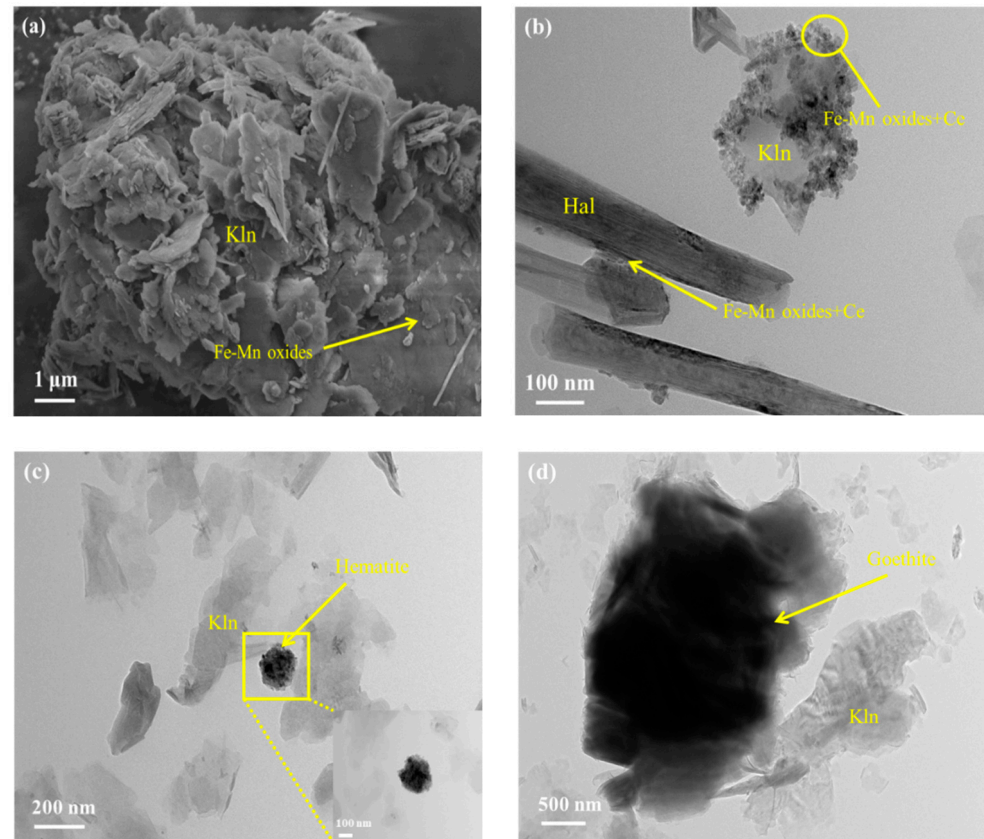


Figure 8. Process of cerium fixation by iron–manganese oxide.

Figure 8 depicts the fixation of cerium onto iron and manganese oxides. In the process of migration and enrichment, rare earth ions were adsorbed by iron–manganese oxide,

and the element cerium was oxidized to four valence states by the oxidation of iron–manganese oxides. Therefore, cerium was strongly bound to the iron–manganese oxide. The remaining rare earth elements were not easily fixed on the iron–manganese oxide and continued to migrate. We further observed the microstructure characteristics of the iron oxide clay mineral complexes in fine particle fractions using scanning electron microscopy and transmission electron microscopy. The results are shown in Figure 9.



**Figure 9.** Microstructure characteristics of Fe–Mn state rare earth. Kln = kaolinite and Hal = halloysite. (a) Surface microstructure of Fe–Mn oxide state rare earth ores; (b–d) Transmission electron microscopy analysis of Fe–Mn oxide state of rare earth ores.

Through the microscopic characterization of the Fe–Mn oxide state from fractional extraction products, it can be found that Fe–Mn oxides were attached to the surface of lamellar kaolinite sheets as globular aggregates (Figure 9a). The HRTEM images of the Fe–Mn oxide state indicate that Fe–Mn oxides were adsorbed on the surface of kaolinite and halloysite as nano-particles and formed specific encapsulated nodules with the rare earth element cerium (Figure 9b). Meanwhile, we found iron oxide structures that were similar to hematite and goethite in the TEM results, which may be the main iron oxides in the oxidation state of iron and manganese (Figure 9c–d) [36]. Therefore, these were the reasons why the rare earth element cerium was abnormal in the Fe–Mn oxide state rare earth orebody.

### 3.6. Organic Binding State of the Weathered Crust Elution-Deposited Rare Earth Ores

The rare earth organic binding state was a rare earth occurrence state in which rare earth elements were combined with organic matter in a geological ore-forming environment. This combination could be explained by the complexation reaction between organic matter and rare earth ions or the existence of rare earth elements adsorbed on organic matter, which can be only released under strong oxidation conditions, and its content depends on the content of organic matter. The contents of rare earth elements in the organic binding

state in each weathered layer of the weathered crust elution-deposited rare earth ore are shown in Figure 10a. The proportions of cerium and yttrium in the organic binding state rare earth are shown in Figure 10b.

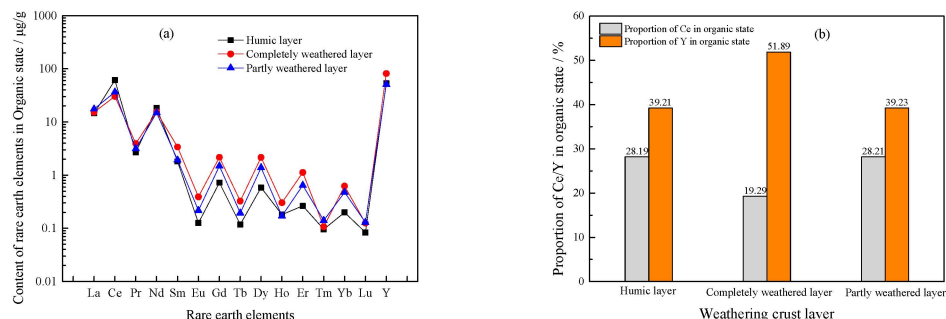


**Figure 10.** Organic binding state of the weathered crust elution-deposited rare earth ore. (a) Content of the organic bound state rare earth elements in each weathered layer; (b) Proportion of Ce and Y in organic bound state in each weathered layer.

It can be seen from Figure 10a that the average contents of rare earth elements in the organic binding state from the humic layer to the partly weathered layer were  $8.66 \mu\text{g}\cdot\text{g}^{-1}$ ,  $10.48 \mu\text{g}\cdot\text{g}^{-1}$  and  $8.65 \mu\text{g}\cdot\text{g}^{-1}$ , respectively, in which the main rare earth elements were cerium and yttrium. According to Figure 10b, cerium accounted for 28.19%, 19.29% and 28.21%, and yttrium accounted for 39.21%, 51.89% and 39.23% from the humic layer to the partly weathered layer, respectively. The active microorganisms in the soil produced a large amount of organic matter, such as humic acid and protein, which led to the enrichment and differentiation of rare earth elements on the mineral surface [37]. Humic acid was the most common organic composition in the surface environment. Humic acid was adsorbed with rare earth ions in a ternary complexation form [15]. In particular, the coordination stability constant and capacity of cerium and yttrium with humic acid were much higher than those of other rare earth elements, resulting in the abnormal phenomenon in the organic binding state [34,38]. Meanwhile, soluble rare earth ions were adsorbed by organic matter and fixed in organic phase, thus the content of these rare earth ions was small [34]. Scanning electron microscopy and transmission electron microscopy were used to detect and analyze the organic binding state of the continuous fractional extraction products, and the results are shown in Figure 11.

As can be seen from Figure 11, the scanning electron microscopy results (Figure 11a) showed that there were a large number of flocculent substances and micro-nano particles adsorbed on the surface of kaolinite, and the scanning electron microscopy energy spectrum results (Figure 11b) showed that these substances mainly contained elements such as O, Si, Al, Fe, Y and Ce. According to the results of transmission electron microscopy (Figure 11c,d), there were a large number of flocculent structures in the organic binding state, which were adsorbed on the surfaces and gaps of kaolinite and halloysite. The rare earth elements yttrium and cerium were the main rare earth ions in the organic binding state, which could be released under strong oxidizing conditions. Meanwhile, it can be seen from Figure 11c,d that a small amount of iron-manganese nodules were observed in the organic binding state, which may be part of the iron-manganese materials left by organic wrapping in the continuous fractional extraction process.

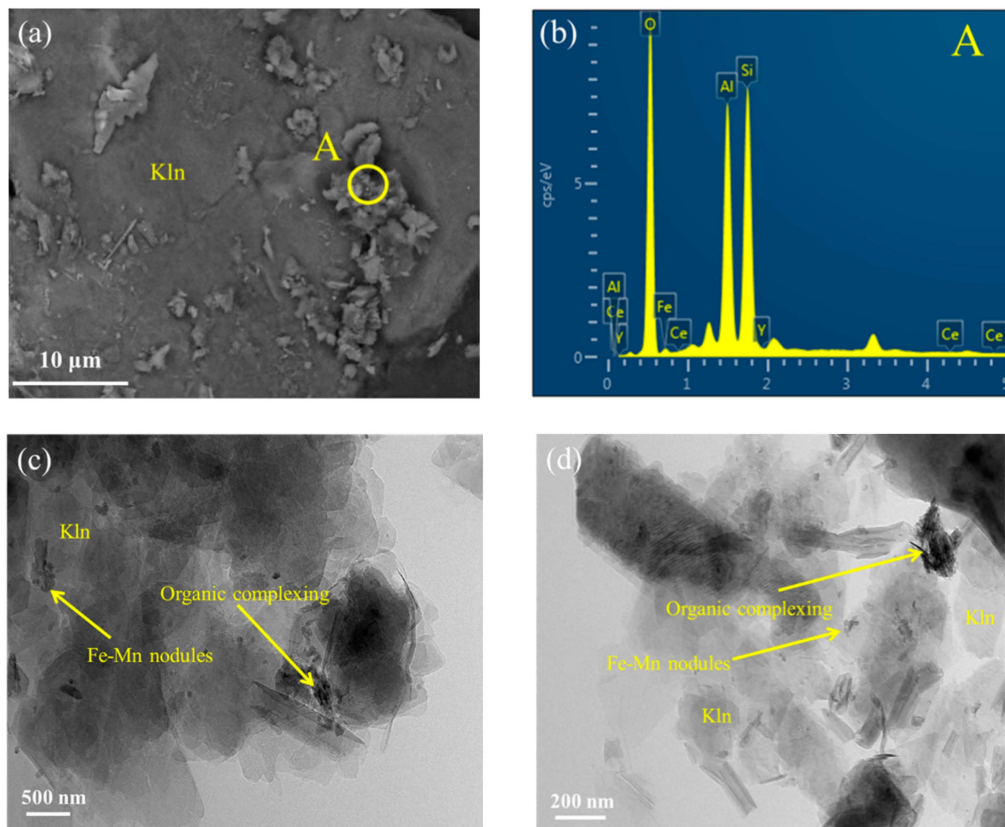


**Figure 11.** Microstructure characteristics of rare earth organic binding state, Kln = kaolinite. (a) Surface microstructure of organic binding state of rare earth ores; (b) Results of energy spectrum analysis at point A; (c,d) Transmission electron microscopy analysis of organic binding state of rare earth ores.

### 3.7. Residual State of the Weathered Crust Elution-Deposited Rare Earth Ores

The rare earth residual state mainly refers to the un-weathered ores in the mineralization process of the weathered crust elution-deposited rare earth ores. This kind of rare earth state mainly inherits the REE distribution of the original rock, and the residual rare earth state is usually difficult to utilize. The differentiation characteristics of rare earth elements in the residual state of different weathering crust layers of the weathered crust elution-deposited rare earth ores in southern Yunnan are shown in Figure 12.

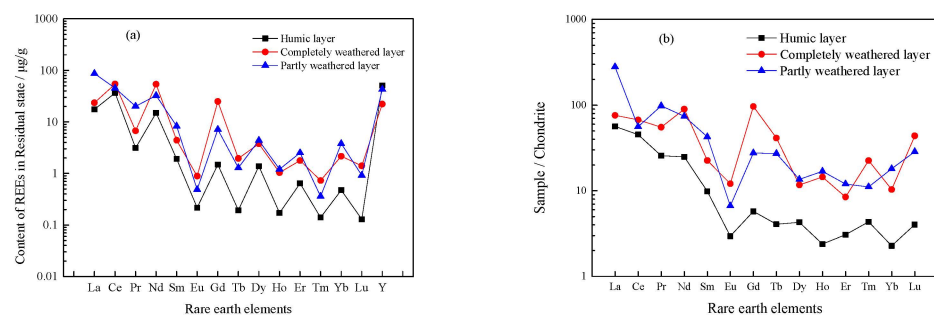


**Figure 12.** Contents of rare earth in residual state and chondrite standards. (a) Content of residual state rare earth elements in each weathered layer; (b) Standard for residual state rare earth element chondrites in each weathered layer.

It can be seen from Figure 12a that the content order of rare earth elements in the residual state was partly weathered layer > completely weathered layer > humic layer, and the average contents were  $258.16 \mu\text{g}\cdot\text{g}^{-1}$ ,  $203.84 \mu\text{g}\cdot\text{g}^{-1}$  and  $129.88 \mu\text{g}\cdot\text{g}^{-1}$ , respectively. The content of rare earth elements in the residual state mainly depended on the weathering degree of the ore. The partly weathered layer showed the highest content of rare earth elements in the residual state because of incomplete weathering and fewer secondary minerals [14]. Combined with the standards of the residual rare earth chondrites, it can be seen that the residual rare earth elements in the humic layer were mainly heavy rare earth elements, the residual rare earth elements in the completely weathered layer were mainly heavy rare earth elements, and the residual rare earth elements in the partly weathered layer were primarily light rare earth elements. Therefore, the release of rare earth elements had an obvious sequence in the weathering process. The light rare earth elements were first released, but the cerium element was abnormal due to its special properties, followed by the liberation of medium and heavy rare earth elements, which further migrate and accumulate.

#### 4. Conclusions

In this paper, the rare earth occurrence states of weathered crust elution-deposited rare earth ores were discussed using the sequential extraction procedure. The occurrence and differentiation characteristics of rare earth elements in the ion exchange state, carbonate bound state, iron–manganese state, organic binding state and residual state in different weathering crust layers were analyzed.

The order of the rare earth element content was completely weathered layer > humic layer > partly weathered layer. LREEs were relatively enriched in the upper part of the weathering crust, while HREEs were relatively enriched in the lower part of the weathering crust. Rare earth elements mainly exist in the ion exchange state. With the deepening of the weathering profile, the degree of weathering gradually decreases, and the content of elements in the ion exchange state gradually decreases. The contents of rare earth elements in the ion exchange state from the top to the bottom of the weathering profile were 78.55%, 73.53% and 53.88%, respectively. In the ion exchange state, all the weathering crust layers showed an obvious cerium anomaly and a certain europium anomaly. The content of rare earth elements in the carbonate bound state was very small, and the rare earth partition pattern was basically consistent with that of the ion exchange state, which had little effect on rare earth element differentiation. The iron–manganese oxide state was mainly enriched with the element cerium, and the content of cerium increased with the depth of the weathering crust. The iron–manganese oxide state was the main factor causing the occurrence of the cerium anomaly. Scanning electron microscopy and transmission electron microscopy analysis showed that Fe–Mn oxides adsorb on the surface of kaolinite and halloysite, or fill in the gaps in the form of micro and nano particles, forming specific nodules with cerium; this shows the abnormal phenomenon of cerium. Meanwhile, the iron oxides in the iron–manganese oxide state were mainly hematite and goethite. The content of rare earth elements in the organic binding state decreased with the deepening of the weathering profile and was mainly related to the content of organic matter in the geological environment. In the organic binding state, rare earth elements were mainly enriched in yttrium and cerium, and rare earth ions were adsorbed on clay minerals through complexation with organic matter. Electron microscopic analysis showed that the surface of the organic binding state contains a large amount of floccule material, and that rare earth ions were combined with floccule material. The rare earth residual state reflects the differentiation characteristics of rare earths elements in the primary rocks. In the process of weathering, light rare earth elements were preferentially released, but cerium elements were abnormal due to their special properties; this was followed by the release of medium and heavy rare earth elements, thus prompting further migration, enrichment and mineralization. The results of this study clarify the occurrence states of rare earth elements in weathered crust elution-deposited rare earth ore and provide new information regarding the benefits of mining these types of rare earth minerals.

**Author Contributions:** Z.Z. and R.C. conceived and designed the experiments; W.C. and F.L. performed the experiments; W.C. and Z.C. analyzed the data; R.C. and Z.Z. contributed reagents/materials/analysis tools; W.C. wrote the paper. All authors have read and agreed to the published version of the manuscript.

**Funding:** This research was funded by National Nature Science Foundation of China (92162109, 52222405, 52074195 and 91962211) and Graduate Innovative Fund of Wuhan Institute of Technology (CX2022570).

**Data Availability Statement:** Not applicable.

**Acknowledgments:** Thanks for the great effort by the editors and reviewers.

**Conflicts of Interest:** The authors declare no conflict of interest.

## References

1. Chai, X.W.; Li, G.Q.; Zhang, Z.Y.; Chi, R.A.; Chen, Z. Leaching kinetics of weathered crust elution-deposited rare earth ore with compound ammonium carboxylate. *Minerals* **2020**, *10*, 516. [\[CrossRef\]](#)
2. Zhang, Z.Y.; He, Z.Y.; Yu, J.X.; Xu, Z.G.; Chi, R.A. Novel solution injection technology for in-situ leaching of weathered crust elution-deposited rare earth ores. *Hydrometallurgy* **2016**, *164*, 248–256. [\[CrossRef\]](#)
3. Chen, Z.; Zhang, Z.Y.; Liu, D.F.; Chi, X.W.; Chen, W.D.; Chi, R.A. Swelling of clay minerals during the leaching process of weathered crust elution-deposited rare earth ores by magnesium salts. *Powder Technol.* **2020**, *367*, 889–900. [\[CrossRef\]](#)
4. Zhang, Z.Y.; He, Z.Y.; Xu, Z.G.; Yu, J.X.; Zhang, Y.F.; Chi, R.A. Rare earth partitioning characteristics of China rare earth ore. *Chin. Rare Earths* **2016**, *37*, 121–127. (In Chinese) [\[CrossRef\]](#)
5. Zhang, Z.Y.; Chi, R.A.; Chen, Z.; Chen, W.D. Effects of ion characteristics on the leaching of weathered crust elution-deposited rare earth ore. *Front. Chem.* **2020**, *8*, 605968. [\[CrossRef\]](#) [\[PubMed\]](#)
6. Super large ion adsorption type rare earth ore was found in southern Yunnan. *Gold Sci. Technol.* **2017**, *25*, 6. (In Chinese)
7. He, Z.Y.; Zhang, Z.Y.; Yu, J.X.; Xu, Z.G.; Chi, R.A. Process optimization of rare earth and aluminum leaching from weathered crust elution-deposited rare earth ore with compound ammonium salts. *J. Rare Earths* **2016**, *34*, 413–419. [\[CrossRef\]](#)
8. Braun, I.J.; Pagel, M.; Herbillon, A.; Rosin, C. Mobilization and redistribution of REs and thorium in a syenitic laterite profile: A mass balance study. *Geochim. Cosmochim. Acta* **1993**, *57*, 4419–4434. [\[CrossRef\]](#)
9. Zhang, Z.Y.; Li, H.; Chi, R.A.; Long, F.; Chi, X.W.; Chen, W.D.; Chen, Z. Inhibition on the swelling of clay minerals in the leaching process of weathered crust elution-deposited rare earth ores. *Appl. Clay Sci.* **2022**, *216*, 106362. [\[CrossRef\]](#)
10. Chi, R.A.; Liu, X.M. Prospect and Development of Weathered Crust Elution-Deposited Rare Earth Ore. *J. Chin. Soc. Rare Earths* **2019**, *37*, 129–140. (In Chinese)
11. Zhang, Z.Y.; Sun, N.J.; He, Z.Y.; Chi, R.A. Local concentration of middle and heavy rare earth elements in the col on the weathered crust elution-deposited rare earth ores. *J. Rare Earths* **2018**, *36*, 552–558. [\[CrossRef\]](#)
12. Harlavan, Y.; Erel, Y. The release of Pb and REE from granitoids by the dissolution of accessory phases. *Geochim. Cosmochim. Acta* **2002**, *66*, 837–848. [\[CrossRef\]](#)
13. Huang, Y.F.; He, H.P.; Liang, X.L.; Bao, Z.W.; Tan, W.; Ma, L.Y.; Zhu, J.X.; Huang, J.; Wang, H. Characteristics and genesis of ion adsorption type REE deposits in the weathering crusts of metamorphic rocks in Ningdu, Ganzhou, China. *Ore Geol. Rev.* **2021**, *135*, 104173. [\[CrossRef\]](#)
14. Berger, A.; Janots, E.; Gnos, E.; Frei, R.; Bernier, F. Rare earth element mineralogy and geochemistry in a laterite profile from Madagascar. *Appl. Geochem.* **2014**, *41*, 218–228. [\[CrossRef\]](#)
15. Davranche, M.; Pourret, O.; Gruau, G.; Dia, A. Impact of humate complexation on the adsorption of REE onto Fe oxyhydroxide. *J. Colloid Interface Sci.* **2004**, *277*, 271–279. [\[CrossRef\]](#) [\[PubMed\]](#)
16. Piasecki, W.; Sverjensky, D.A. Speciation of adsorbed yttrium and rare earth elements on oxide surfaces. *Geochim. Cosmochim. Acta* **2008**, *72*, 3964–3979. [\[CrossRef\]](#)
17. Janots, E.; Bernier, F.; Brunet, F.; Munoz, M.; Trcera, N.; Berger, A.; Lanson, M. Ce(III) and Ce(IV) (re)distribution and fractionation in a laterite profile from Madagascar: Insights from in situ XANES spectroscopy at the Ce L-III-edge. *Geochim. Cosmochim. Acta* **2015**, *153*, 134–148. [\[CrossRef\]](#)
18. Li, M.Y.H.; Zhou, M.F. The role of clay minerals in formation of the regolith-hosted heavy rare earth element deposits. *Am. Mineral.* **2020**, *105*, 92–108. [\[CrossRef\]](#)
19. Yusoff, Z.M.; Ngwenya, B.T.; Parsons, I. Mobility and fractionation of REEs during deep weathering of geochemically contrasting granites in a tropical setting, Malaysia. *Chem. Geol.* **2013**, *349*, 71–86. [\[CrossRef\]](#)
20. Braun, J.J.; Riotte, J.; Battacharya, S.; Violette, A.; Oliva, P.; Prunier, J.; Marechal, J.C.; Ruiz, L.; Audry, S. REY-Th-U dynamics in the critical zone: Combined influence of reactive bedrock accessory minerals, authigenic phases, and hydrological sorting (Mule Hole Watershed, South India). *Geochem. Geophys. Geosyst.* **2018**, *19*, 1611–1635. [\[CrossRef\]](#)
21. Duzgoren-Aydin, N.S.; Aydin, A. Distribution of rare earth elements and oxyhydroxide phases within a weathered felsic igneous profile in Hong Kong. *J. Asian Earth Sci.* **2009**, *34*, 1–9. [\[CrossRef\]](#)

22. Li, Y.H.M.; Zhao, W.W.; Zhou, M.F. Nature of parent rocks, mineralization styles and ore genesis of regolith-hosted REE deposits in South China: An integrated genetic model. *J. Asian Earth Sci.* **2017**, *148*, 65–95. [[CrossRef](#)]
23. Fu, W.; Li, X.; Feng, Y.; Peng, M.; Peng, Z.; Yu, H.X.; Lin, H.R. Chemical weathering of S-type granite and formation of Rare Earth Element (REE)-rich regolith in South China: Critical control of lithology. *Chem. Geol.* **2019**, *520*, 33–51. [[CrossRef](#)]
24. Li, M.Y.H.; Zhou, M.F.; Williams-Jones, A.E. The genesis of regolith-hosted heavy rare earth element deposits: Insights from the world-class Zudong deposit in Jiangxi province, south China. *Econ. Geol.* **2019**, *114*, 541–568. [[CrossRef](#)]
25. Fan, W.X.; Zhou, J.M.; Zhang, H.; Liu, D.; Yuan, P. Research progresses and prospects on carrier minerals of rare earth elements (REY) in deep-sea REY-rich sediments. *Acta Mineral. Sin.* **2023**, *43*, 145–156. (In Chinese) [[CrossRef](#)]
26. Wang, F.L.; He, G.W.; Ren, J.B.; Yang, Y.; Deng, X.G. Comparative study on the geochemical characteristics of rare earth elements in deep-sea sediments from different regions of the Pacific Ocean. *Acta Petrol. Sin.* **2023**, *39*, 719–730. (In Chinese) [[CrossRef](#)]
27. Wood, S.A. The aqueous geochemistry of the rare-earth elements and yttrium. *Chem. Geol.* **1990**, *82*, 159–186. [[CrossRef](#)]
28. Huang, J.; Tan, W.; Liang, X.L.; He, H.P.; Ma, L.Y.; Bao, Z.W.; Zhu, J.X. REE fractionation controlled by REE speciation during formation of the Renju regolith-hosted REE deposits in Guangdong Province, South China. *Ore Geol. Rev.* **2021**, *134*, 104172. [[CrossRef](#)]
29. Hou, X.Z.; Yang, Z.F.; Wang, Z.J.; Wang, W.C. The occurrences and geochemical characteristics of thorium in iron ore in the Bayan Obo deposit, Northern China. *Acta Geochim.* **2020**, *39*, 64. [[CrossRef](#)]
30. Lu, Y.F.; Zhang, X.Y.; Zhu, K.Y.; Wang, J.Y.; Yu, M.; Huang, M.; Shi, X.F. Occurrence of Rare Earth Elements and Yttrium (REY) in core sediments from the Central Indian Oceanic Basin (CIOB). *J. Chin. Soc. Rare Earths* **2023**, 1–22. Available online: <http://kns.cnki.net/kcms/detail/11.2365.TG.20220510.1052.004.html> (accessed on 13 October 2022). (In Chinese).
31. GBW07441-07445, Certified Reference Materials for Element Forms in Soils. Beijing, China. 2007.
32. Wang, Z.G.; Yu, X.Y.; Zhao, Z.H. *Rare Earth Elements Geochemistry*; Science Press: Beijing, China, 1989; p. 535.
33. Chen, W.D.; Zhang, Z.Y.; Chi, R.A. Assisted leaching process of weathered crust elution-deposited rare earth ore by ammonium carboxylate. *Metal Mine* **2020**, *5*, 191–196. (In Chinese) [[CrossRef](#)]
34. Geng, A.C.; Zhang, S. Binding capacity and stability of humic acid with rare earth elements in solution. *Chin. Environ. Sci.* **1998**, *1*, 53–57. (In Chinese)
35. Chi, R.A.; Tian, J.; Luo, X.P.; Xu, Z.G.; He, Z.Y. The basic research on the weathered crust elution-deposited rare earth ores. *Nonferrous Met. Sci. Eng.* **2010**, *3*, 1–13. (In Chinese) [[CrossRef](#)]
36. Wu, P.Q.; Zhou, J.W.; Huang, J.; Lin, X.J.; Liang, X.L. Enrichment and fractionation of rare earth elements in ion-adsorption rare earth elements deposits: Constraints of iron oxide-clay mineral composites. *Geochimica* **2022**, *51*, 271–282. (In Chinese) [[CrossRef](#)]
37. Liang, X.L.; Tan, W.; Ma, L.Y.; Zhu, J.X.; He, H.P. Mineral surface reaction constraints on the formation of ion-adsorption rare earth element deposits. *Earth Sci. Front.* **2022**, *29*, 29–41. (In Chinese) [[CrossRef](#)]
38. Chen, Z.C.; Yu, S.J.; Fu, Q.C.; Chen, B.H.; Zhang, L.J. Study on the Organic Metallogenic Mechanism of Weathering Crust REE Deposits. *J. Chin. Soc. Rare Earths* **1997**, *3*, 53–60. (In Chinese)

**Disclaimer/Publisher's Note:** The statements, opinions and data contained in all publications are solely those of the individual author(s) and contributor(s) and not of MDPI and/or the editor(s). MDPI and/or the editor(s) disclaim responsibility for any injury to people or property resulting from any ideas, methods, instructions or products referred to in the content.